Atmospheric Environment 272 (2022) 118939

Contents lists available at ScienceDirect

Atmospheric Environment

journal homepage: www.elsevier.com/locate/atmosenv

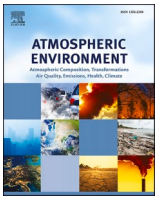

Characterization of particle sources and comparison of different particle metrics in an urban detached housing area, Finland

K. Teinilä [a,*], H. Timonen [a], M. Aurela [a], J. Kuula [a], T. Rönkkö [b], H. Hellèn [a], K. Loukkola [c], A. Kousa [c], J.V. Niemi [c], S. Saarikoski [a]

[a] Atmospheric Composition Research, Finnish Meteorological Institute, Helsinki, Finland
[b] Aerosol Physics Laboratory, Physics Unit, Faculty of Engineering and Natural Sciences, Tampere University, Tampere, Finland
[c] Helsinki Region Environmental Services Authority (HSY), Helsinki, Finland

HIGHLIGHTS

- The sources influencing air quality in detached house area in the Helsinki metropolitan area were characterized.
- Special attention was paid on the parameters that can be utilized to estimate the main particle sources and to assess their impact on air quality.
- Elevated PM1 concentration was attributed especially to the LRT and local wood burning in fireplaces.

ARTICLE INFO

Keywords:
Particulate matter
wood burning
Traffic
Long-range transport
Aerosol chemical composition

ABSTRACT

Particulate matter (PM) is emitted from various anthropogenic sources in urban areas affecting the local air quality. The aim of this study was to characterize the sources influencing air quality in detached house area in the Helsinki metropolitan area in Finland, and secondly, to explore the additional value of new particle physical properties to assess the impact of residential combustion on air quality. Measurements were conducted in an urban detached housing area between January and April 2019. Measured particle physical properties were particle number (PN), particle mass (PM_1) and lung deposited surface area (LDSA) concentrations and number size distributions. In addition, particle chemical composition was measured using a soot particle aerosol mass spectrometer (SP-AMS; organic compounds, inorganic ions) and an aethalometer (black carbon (BC)). Concentrations of selected monosaccharide anhydrides and polycyclic aromatic hydrocarbons were analysed from the PM_{10} filter samples. The sources and characteristics of organic aerosol was investigated by applying positive matrix factorization to the mass spectra measured with the SP-AMS. Based on the variations in the measured particle physical parameters, chemical species and meteorology, the measurement period was divided into three sub periods dominated by urban background, wood burning and long-range transport (LRT) aerosols. Highest pollutant concentrations were measured during the wood burning and LRT periods. Wood burning increased the concentrations of all measured species, but the differences were most significant to levoglucosan, benzo(a) pyrene, BC and PM_1 that had 12, 10, 6.4 and 3.6 times larger mean concentrations during the wood burning period compared to the urban background period, respectively. LRT affected significantly levoglucosan, PM_1 and BC concentrations, since LRT pollutants partly originated from open biomass fires in Eastern Europe. The impact of local wood burning and LRT was quite small to particle number concentrations, whereas LDSA concentrations and size distributions were affected by traffic, wood combustion emissions and LRT. BC concentration correlated with the LDSA concentration during all periods suggesting a common origin. Particle number concentration was a good indicator of local combustion, especially traffic emissions, while the PM_1 mass concentration together with secondary particle material was a good measure for the LRT pollutants. Benzo(a)pyrene was found to be a good indicator of local wood burning, but it was not detected in LRT biomass combustion particles.

* Corresponding author.
E-mail address: kimmo.teinila@fmi.fi (K. Teinilä).

https://doi.org/10.1016/j.atmosenv.2022.118939
Received 4 August 2021; Received in revised form 27 December 2021; Accepted 4 January 2022
Available online 5 January 2022

1. Introduction

Particulate matter (PM) emitted from anthropogenic sources affects air quality and is connected to negative health effects (Lelieveld et al., 2015; Atkinson et al., 2014). Especially fine particles ($PM_{2.5}$, particles smaller than 2.5 μm in diameter) and sub-micron particles are considered harmful as they can be transported deep into the human respiratory tract (Zanobetti et al., 2014). Particles also contribute to climate change by scattering and absorbing incoming solar radiation and indirectly via cloud processing. Black carbon (BC) in particular absorbs solar radiation and has a positive radiative forcing effect.

$PM_{2.5}$ concentration is currently one of the key parameters to assess air quality in air quality monitoring networks across the globe. However, in most cases $PM_{2.5}$ does not provide information on the sources and properties of particles. There are several currently unregulated particulate parameters that have high potential to complement long-term monitoring of anthropogenic particles and elucidate particle sources and their influences on climate and health. In terms of health impacts, elevated particle number (PN) concentrations and BC have been connected to the adverse health effects. Ultrafine particles, i.e., particles smaller than 100 nm and representing majority of PN, can cause more pulmonary inflammation and are retained longer in the lungs than $PM_{2.5}$ (Schraufnagel, 2020). Lung deposited surface area (LDSA) is one measure for the harmfulness of particles as it represents the potential for toxic chemicals on the surfaces of particles to enter the human respiratory and blood circulating system (Brown et al., 2001; Oberdörster et al., 2005). LDSA concentrations are mainly driven by particles smaller than 400 nm, and much of the LDSA in urban areas typically originates from vehicular exhaust emissions and residential wood combustion (Tissari et al., 2008; Karjalainen et al., 2016; Kuuluvainen et al., 2016; Kuula et al., 2020b).

Regarding chemical species in particles, BC is a product of incomplete combustion, typically emitted by engines, residential burning or industrial processes. BC is in relatively small particle sizes, and may have negative health effects by itself, but chemical components entering to human body together with BC particles (soot) may also be toxic or carcinogenic, like polycyclic aromatic hydrocarbons (PAH) (Jansen et al., 2011; Luben et al., 2017 and references therein). Local wood burning is a source of PAH compounds, one of the most important PAH species being benzo(a)pyrene (Guereiro et al., 2015; Hellén et al., 2017). Benzo(a)pyrene has been regarded as a marker for both the total and carcinogenic PAHs (EU directive, 2004). However, there is some evidence that other PAHs (e.g. dibenz(a,h)anthrasene) may have even higher health risk than benzo(a)pyrene (Lammel, 2015).

Based on the previous studies, the main local anthropogenic fine particle sources in the Helsinki metropolitan area are direct vehicular emissions and residential wood burning (Aurela et al., 2015; Carbone et al., 2013; Saarikoski et al., 2008; Järvi et al., 2008; Pirjola et al., 2017). Other anthropogenic sources affecting PM concentrations are e.g., road dust, energy production and ship emissions (Kupiainen et al., 2016; Soares et al., 2014). The Helsinki metropolitan area is also affected by long-range transported (LRT) pollution episodes, during which the concentration of fine particulate matter is significantly elevated. These episodes are typically due to the anthropogenic emissions from Central and Eastern Europe or regional or LRT smoke plumes from forest fires or agricultural burning (Leino et al., 2014; Niemi et al., 2004, 2005, 2009; Pirjola et al., 2017). Additionally, PM can be increased due to the wintertime inversion when locally produced pollutants are trapped in the planetary boundary layer over the city (Barreira et al., 2021; Teinilä et al., 2019).

The aim of this study is to characterize the sources affecting air quality in an urban detached housing area, Finland, and identify the additional parameters that needs to be measured in order to characterize better the impact of these sources on air quality. Special attention is paid on the parameters that can be monitored in real-time in the air quality monitoring networks i.e., particle number, LDSA and BC concentrations. To support the characterization of the sources, Soot Particle Aerosol Mass Spectrometer (SP-AMS) measurements were carried out at the site and the data was analysed with a Positive Matrix Factorization (PMF) method. Additionally, daily PM_{10} filter samples were analysed for biomass burning markers, monosaccharide anhydrides (MAs), as well as for PAHs. Earlier studies in the Helsinki metropolitan area (e.g., Kuula et al., 2020a; Luoma et al., 2021; Pirjola et al., 2017; Aurela et al., 2015) have found differences between the sources, concentrations and chemical composition of particulate matter at the sites which represent different urban environments. In this study, we focus on the detailed characterization of particle physical and chemical properties and sources by using the real time instruments as well as PM_{10} filter samples. This information will be further utilized to explore the monitoring parameters needed to be measured in order to assess the impact of these sources on air quality. The results presented in this study are necessary for the authorities when assessing the climate and air quality impacts of anthropogenic particulate sources as well as directing the emission legislation and emission mitigation actions. Although the measurements were performed only at one location in Helsinki, Finland, the results are also applicable to other similar areas.

2. Experimental

2.1. Measurement site

Measurements were conducted at a residential suburban area in Helsinki, Finland (Fig. S1). The intensive campaign was conducted between January 15 and April 16, 2019 (a 3-month campaign). Measurement station, maintained by the Helsinki Region Environmental Services Authority (HSY), was located next to a small street in Pirkkola detached housing area (60.234211N, 24.922591E, Kuula et al., 2020a). The Pirkkola area is characterized by small, detached houses of which majority have fireplaces. Fireplaces are typically used for supplementary heating during cold seasons, heating of sauna stoves and decorative burning. With regard to traffic, there are some small and medium size streets (traffic volumes from hundreds to thousands of vehicles per day) at the area that can have an influence on the pollutants measured at the site. The distance to the closest main road is ~600 m from the measurement site, and the distance to other two main roads are 1 km in the directions of West, North and East. The corresponding traffic rates in these roads were 43500, 103000, and 42700 vehicles per day in 2019 (Finnish Transport Infrastructure Agency, 2019).

2.2. Soot Particle Aerosol Mass Spectrometer (SP-AMS)

The concentrations of organics, sulphate, nitrate, ammonium and chloride were determined with the Soot Particle Aerosol Mass Spectrometer (Aerodyne Research Inc, Billerica, US; Onasch et al., 2012). The SP-AMS was operated with a time-resolution of ~90 s of which half of the time was measured in the mass spectra mode (mass concentrations) and half of the time in Particle Time-of-Flight mode (PToF; size distributions). Because of the aerodynamic lens system, the size range covered by the SP-AMS was approximately from ~50 nm to 1 μm. The SP-AMS is different from the standard AMS since it has an additional laser vaporizer that allows the determination of refractory particulate species. However, in this paper, the results from the refractory material, i.e., refractory black carbon (rBC), are shown only for the mass size distributions. The SP-AMS data was analysed with IGOR 6.37 SQRL 1.62A and PIKA 1.22A software. A collection efficiency of one was applied to the data set. Polycyclic aromatic hydrocarbons (total PAH concentration) were extracted from the SP-AMS data with the method described by Dzepina et al. (2007).

The sources of organic aerosol (OA) were investigated by analyzing the high-resolution mass spectra of organics with Positive Matrix Factorization (PMF; CU AMS PMF tool v. 2.08D, Paatero and Tapper, 1994; Ulbrich et al., 2009). The details of the PMF analysis are given in

another paper (Saarikoski et al., 2021), and therefore, the PMF analysis is described here only shortly. Before the PMF analyses, the data was averaged to 10 min. The number of factors was investigated from two to eight of which the solution with five factors described the characteristics and variation of organic matter most realistically. The factors were identified as hydrocarbon-like organic aerosol (HOA), biomass burning OA (BBOA), semi-volatile oxygenated OA (SV-OOA), low-volatility oxygenated OA (LV-OOA) and LV-OOA from the long-range transport (LV-OOA-LRT). HOA showed a classic hydrocarbon pattern of engine emissions with the largest signals for $C_3H_5^+$, $C_3H_7^+$, $C_4H_7^+$, $C_4H_9^+$, $C_5H_9^+$ and $C_5H_{11}^+$ at mass to charge ratio (m/z) of 41, 43, 55, 57, 69 and 71 (Canagaratna et al., 2004), respectively, and had a high hydrogen to carbon ratio (H:C) and low oxygen to carbon ratio (O:C). HOA also correlated strongly with NO (square of Pearson correlation coefficients (R^2) = 85) and NOx (R^2 = 0.88) indicating that it originated mostly from vehicle emissions. The mass spectra of BBOA displayed signal for $C_2H_4O_2^+$ and $C_3H_5O_2^+$ at m/z 60 and 73, respectively, that are typical fragments for biomass burning emissions (Alfarra et al., 2007). The time trend of BBOA was compared to that of monosaccharide anhydrides (MAs: levoglucosan, mannosan and galactosan) analysed from the 24-h PM_{10} filter samples. R^2 between BBOA and levoglucosan, mannosan and galactosan were 0.95, 0.92 and 0.84, respectively. Also chloride had the strongest correlation with BBOA (R^2 = 0.40).

LV-OOA had the highest signal for CO_2^+ and CO^+ at m/z 44 and 28, respectively, and was highly oxygenated with a large O:C, while SV-OOA was less oxidized showing the largest signal for $C_2H_3O^+$ at m/z 43. Inorganic species measured by the SP-AMS, sulphate, nitrate and ammonium, correlated strongest with LV-OOA (R^2 = 0.40, 0.32 and 0.45, respectively). LV-OOA-LRT had very similar mass spectra to LV-OOA but their time-series and diurnal trends were different. LV-OOA-LRT was observed mostly at the end of the measurement period in April when a strong LRT episode with an elevated PM_1 concentration was detected at the site. Based on the NAAPS model results and calculated air mass back trajectories, smoke aerosol arrived in Helsinki from open fires in Eastern Europe. LRT episode will be studied in detail in Section 3.2.3. For the validation purposes, the PMF solution of five factors was examined for the rotational freedom by varying fpeak and for accuracy with bootstrapping tests and multiple seeds.

2.3. Aethalometer

A dual-spot aethalometer (AE33, Magee Scientific, Slovenia, (Magee Scientific, 2016)) was used to measure aerosol light absorption and corresponding black carbon mass concentration at seven different wavelengths between 370 and 950 nm (Hansen et al., 1984; Drinovec et al., 2015). The flow rate of the aethalometer was 5 l min^{-1}. The filter tape used was a PTFE-coated glass fibre filter (no. M8020). The cut-off size of the sample was 1 μm, and it was achieved using a sharp cut cyclone (Model SCC1.197, BGI Inc., Butler, NJ, USA) in the inlet. The multiple scattering enhancement factor C of 1.57 was utilized (Drinovec et al., 2015), and the default the mass absorption coefficient (MAC) values were used. The concentrations of fossil fuel (BC_{ff}) and wood burning (BC_{wb}) related BC were calculated using Sandradewi et al. (2008) model with the Angstrom exponent values of 0.9 for fossil fuel and 1.68 for wood burning (Zotter et al., 2017).

2.4. Other particle and gas instrumentation

Particle size distributions in mobility size range of 15–685 nm were measured with a Scanning Mobility Particle Sizer (SMPS) consisting of a differential mobility analyser (DMA; model 3080, TSI Inc., USA) and a condensation particle counter (CPC; model 3775, TSI Inc., USA). Particle mass concentration was measured with a GRIMM Aerosol Spectrometer (model 1.108, 15 channels, 0.23–20 μm). In the further discussion, the PM_1 concentration is obtained from the GRIMM Aerosol Spectrometer. Particle number concentration (PN, particles larger than 5 nm) was measured using a CPC A20 (Airmodus). Concentration of lung deposited surface area of particles (LDSA) was measured using an AQ™ Urban instrument (10–400 nm size range, Pegasor). Additionally, the size distribution of LDSA was calculated from the SMPS data by weighing the number size distribution with the particle size-specific deposition fraction and then calculating the total surface area of particles accordingly. Particle size-specific deposition fractions are presented in a report published by the International Commission on Radiological Protection (ICRP, 1994).

NO, NO_x and NO_2 were measured with a minute time-resolution with a Horiba APNA 370. Wind speed and direction were measured with WMT 703 (Vaisala) and temperature and RH were measured with HMP 155 (Vaisala) at the Pasila meteorological station, 4 km south of the Pirkkola site. Furthermore, $PM_{2.5}$ results (FH 62 I-R; ESM Andersen Instruments, GmbH, Germany) from the regional background site (Luukki) were utilized to characterize the contributions of LRT particle concentrations. All the particle, gas and meteorological data were averaged for hourly results.

Back trajectories of air masses arriving in the measurement site were calculated using the NOOA HYSPLIT model (Stein et al., 2015; Rolph et al., 2017). The 96-h back trajectories were calculated for every hour for 200 m above sea level. The data analysis was made using the R software (R Core Team, 2020) and R package openair (Carslaw and Ropkins, 2012). The Navy Aerosol Analysis and Prediction System (NAAPS) model results were used to determine the distribution of LRT smoke aerosols from open biomass burning (http://www.nrlmry.navy.mil/aerosol/; the Naval Research Laboratory, Monterey, CA, USA).

2.5. PM_{10} filtersampling and analyses

A total of 89 24-h PM_{10} filter samples were collected at the measurement site during the 3-month long campaign. The concentration of monosaccharide anhydrides (levoglucosan, mannosan and galactosan) were analysed from the PM_{10} samples using a high-performance anion-exchange chromatography-mass spectrometry (HPAEC-MS). The HPAEC-MS system consists of a Dionex ICS-3000 ion chromatograph coupled with a quadrupole mass spectrometer (Dionex MSQ). The HPAEC–MS system had 2 mm CarboPac PA10 guard and analytical columns (Dionex) and potassium hydroxide (KOH) eluent. The used ionization technique was electrospray ionization. The analytical method is similar to that described in Saarnio et al., 2010a,b, except that the used internal standard was methyl-β-D-arabinopyranoside. Half of the 47 mm filters were extracted into 10 mL of MQ water with internal standard concentration of 100 ng mL^{-1}, and the HPAEC-MS was utilized for the determination of MAs at m/z 161. The uncertainty of the analyses was typically 10–15% and even larger (25%) when the analysed concentration was low.

The concentrations of 6 PAHs (benzo(a)anthracene, benzo(b)fluoranthene, benzo(k)fluoranthene, benzo(a)pyrene, indeno(1,2,3-cd) pyrene, dibenz(a,h)anthracene) were analysed from the PM_{10} samples using a gas chromatograph-mass spectrometer (GC-MSMS, Agilent 7890A and 7010 GC/MS Triple Quadrupole). For the analysis, the samples were usually pooled together as monthly samples, ultrasonic extracted with toluene, dried with sodium sulphate and concentrated to 1 mL. For chromatographic separation, the HP-5MS UI column (30mx0.25 mm i.d., film thickness 0.25 μm) and 2m pre-column (same phase as analytical column) were used. Helium (99.9996%) was used as a carrier gas with a flow of 1 mL min^{-1}. The temperature program started at 60 °C with a 1 min hold, followed by an increase of 40 °C min^{-1} to 170 °C, and 10 °C min^{-1} to 310 °C with a hold of 3 min. Deuterated PAH compounds (Naphthalene-d8, Acenaphthene-d10, Phenanthrene-d10, Chrysene-d12, Perylene-d12, PAH-Mix 31D, Dr. Ehrenstorfer) were used as internal standards and were added to an extraction solvent before extraction. External standards (PAH Mix-137, Polynuclear aromatic hydrocarbons Mix, Dr. Ehrenstorfer) with five different concentration levels were used. In the analysis of BaP, EN

15549 (2008) standard was followed. Measurement uncertainty was calculated from the validation data (Guide Nordtestin TR537) for the target value (0.1 ng m^{-3}) that value was found to be 25%. The analysis method is accredited (SFS-EN ISO/IEC 17025:2017). The method has been previously described in detail by Vestenius et al. (2011).

The measured chemical and physical properties of particulate matter together with the obtained factors from the PMF analysis, meteorology, air mass trajectories and NAAPS model results were used to divide the measurement period into three subperiods (section 3.2). The chosen periods were urban background period with no significant pollutant sources, wood burning period when impact of local wood burning was significant, and a long-range transport period when air quality was influenced by long-range transport.

3. Results and discussion

3.1. General description of the measurement period

Mean temperature and relative humidity during the three-month measurement campaign (Jan 15th- April 16th) were −0.5 °C and 77%, respectively (Fig. S2). Wind speed was relatively low during the measurement campaign, being on average 4.5 m s^{-1} (max. hourly mean 11.3 m s^{-1}), and the prevailing wind direction was in the sector South-West to North-West. Wind speed showed nearly no diurnal variation in January, but from February to April, there was a clear diurnal variation with maximum values during daytime. The difference between wind speed during day and night was most notable in April, although the day-night difference was on average only ~1 m s^{-1}. Temperature showed distinctive diurnal pattern only in April. The mean diurnal variations of temperature, relative humidity, and wind speed during the measurement period are shown in Fig. S3.

The mean fine particulate matter (PM_1) concentration was 6.6 μg m^{-3} during the measurement period (Table 1, Fig. 1) with the highest 1-h mean PM_1 concentration being 73 μg m^{-3}. The largest PM_1 concentrations were measured during the coldest days of the measurement period in January. Elevated PM_1 concentrations in detached house areas during cold season are typically connected to increased wood burning for heating purposes and poor dilution and mixing of pollutants due to stagnant meteorological conditions (temperature inversion). In general, the mean PM_1 concentration measured in this study was similar to the $PM_{2.5}$ concentrations measured in detached house areas in the Helsinki metropolitan area by Luoma et al. (2021) and Helin et al. (2018), but lower than those measured by Aurela et al. (2015).

Table 1
Mean concentrations of selected particle physical parameters and chemical species during the whole measurement period in 2019 and subperiods selected for the detailed investigation (urban background, wood burning, LRT, see section 3.2). MA concentration is the sum of measured monosaccharide anhydrides (levoglucosan, mannosan and galactosan) and inorganic ions concentration is the sum of sulphate, nitrate, ammonium and chloride.

	Whole period	Urban background	Wood burning	LRT
	15.01 00:00–16.04. 23:00	18.03 00:00–31.03. 23:00	15.01 00:00–31.01. 23:00	04.04 06:00–09.04 14:00
PM_1 (μg m^{-3})	6.58	3.06	10.91	14.57
PN (p cm^{-3})	7086	6066	9748	8203
LDSA (μm^2 cm^{-3})	9.67	5.97	16.19	18.23
BC (μg m^{-3})	0.71	0.26	1.69	1.06
NO_x (μg m^{-3})	24.0	12.0	57.5	32.0
Benzo(a) pyrene (ng m^{-3})	0.85	0.26	2.71	0.34
MA (μg m^{-3})	0.14	0.03	0.40	0.22
Organics (μg m^{-3})	2.94	1.35	4.91	9.89
Inorganic ions (μg m^{-3})	1.30	0.64	2.18	2.37

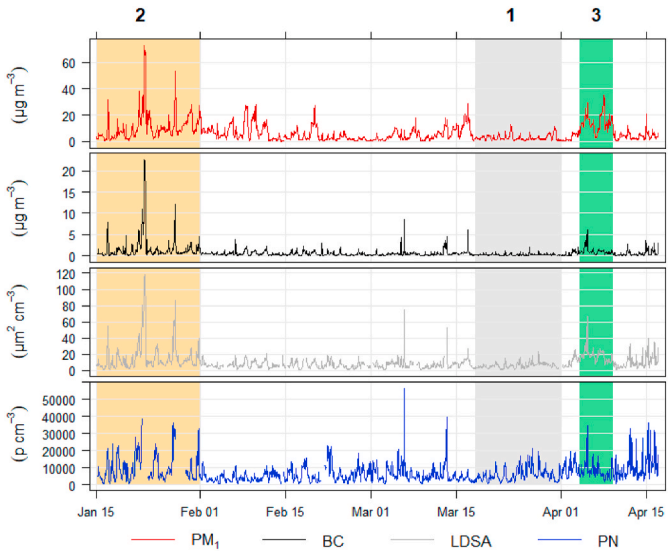

Fig. 1. Time series of hourly mean PM_1, BC, LDSA and PN concentrations during the measurement period. The subperiods selected for detailed investigation (section 3.2) are highlighted by different colours and numbers (2 wood burning = orange, 1 urban background = grey, 3 LRT = green). (For interpretation of the references to colour in this figure legend, the reader is referred to the Web version of this article.)

The mean concentrations of BC, PN and NO_x were 0.7 μg m^{-3}, 7086 particles cm^{-3} and 24 μg m^{-3}, respectively, during the measurement period (Table 1.) The highest measured hourly mean concentrations for BC (22.6 μg m^{-3}) and NO_x (863 μg m^{-3}) were measured in January together with the highest PM_1 concentrations. The mean BC concentration was at the same level to that reported for similar environments by Luoma et al. (2021) and Helin et al. (2018). Also, the largest concentrations of PN were measured in January (mean 9750 and max hourly mean 38 750 particles cm^{-3}), but the PN concentrations were also high in April (mean 9 565 and max 36 400 particles cm^{-3}).

The mean diurnal variations of PM_1, PN, NO_x and BC are shown in Fig. S4. PM_1 did not show very strong variation throughout the day, although PM_1 concentration was elevated in the evenings that may indicate local or regional wood burning source. Additionally, a slight increase in PM_1 was observed in the morning. This increase is most likely connected to increased traffic frequency during morning rush hour which typically takes place between 7 and 9 a.m. in the Helsinki city area (Luoma et al., 2021). PN and NO_x showed clearly higher concentrations in the morning (maximum between 9 and 10 a.m.). In urban areas, PN and NO_x are typically connected to motor vehicle related emissions (Pirjola et al., 2017). The afternoon rush hour peak for PN was clearly smaller compared to the morning peak when the whole measurement period was taken account, but it was more evident when the measurement period was divided into sub periods (section 3.2). It is possible that the PN concentration connected to traffic was more sensitive to the meteorological conditions like wind speed, wind direction and mixing height since the traffic related pollutants were partly transported to the measurement site from the main roads ~1 km distance. However, the diurnal trends of the traffic related pollutants were mostly caused by local traffic at nearby smaller streets. BC had also elevated concentrations during the morning rush hour, but the largest

BC concentrations were measured in the evening between 7 and 11 p.m. The existence of the late evening BC peak during the whole measurement period indicates that its origin was probably the local wood burning.

The mean LDSA concentration was 9.7 $\mu m^2\ cm^{-3}$ during the measurement period (Fig. 1), and the highest 1-h mean LDSA concentration during the measurement period was 119 $\mu m^2\ cm^{-3}$. The mean LDSA concentration was very similar to that reported by Kuula et al. (2020b) in another detached housing area (12 $\mu m^2\ cm^{-3}$), but clearly lower than in a busy street canyon (22 $\mu m^2\ cm^{-3}$) in the Helsinki metropolitan area. High LDSA concentrations were measured in January together with the highest PM_1 and BC concentrations and in April which was identified as a LRT period (section 3.2). The diurnal variation of the LDSA concentration during the whole measurement period showed two peaks, one in the morning and one in the late evening (Fig. S5). The morning peak coexisted with NO_X, BC and PN peaks and the late evening peak with PM_1 and BC peaks. The diurnal variation of LDSA was similar to that measured by Kuula et al. (2020b) in the detached house area during cold season.

Mean concentrations of organics, sulphate, nitrate, and ammonium measured with the SP-AMS were 2.9 $\mu g\ m^{-3}$, 0.6 $\mu g\ m^{-3}$, 0.4 $\mu g\ m^{-3}$ and 0.2 $\mu g\ m^{-3}$, respectively (Fig. S6). The sum of the concentrations of the measured chemical components (organics and inorganic ions from SP-AMS and BC from aethalometer) showed high correlation against PM_1 ($R^2 = 0.8$) and the total particle volume measured with the SMPS ($R^2 = 0.9$). The diurnal cycles of the chemical components measured with the SP-AMS are shown in Fig. S7. Secondary inorganic aerosol components, sulphate, nitrate and ammonium, did not show any clear diurnal cycle, but chloride showed a slight increase towards afternoon and evening. This may indicate wood burning being one of its sources, however, the mean concentration of chloride was very low during the measurement period (36 ng m^{-3}). Significantly higher chloride concentrations are typically measured in polluted areas (e.g., Gani et al., 2019; Carbone et al., 2013). The diurnal variation of organics was similar to that of BC indicating similar sources of these two aerosol components.

Mean concentration of MAs (sum of levoglucosan, mannosan and galactosan) calculated from the 24-h filter samples was 0.14 $\mu g\ m^{-3}$ (Table 1, Fig. 2). Levoglucosan constituted the largest portion of MAs (83%) followed by mannosan (11%) and galactosan (6%). The mean concentration of benzo(a)pyrene was 0.85 ng m^{-3} during the measurement campaign. Concentrations of other studied PAHs had very high correlation coefficient with benzo(a)pyrene ($R^2 > 0.98$), except dibenz(a,h)anthracene for which R^2 was a bit lower (0.90).

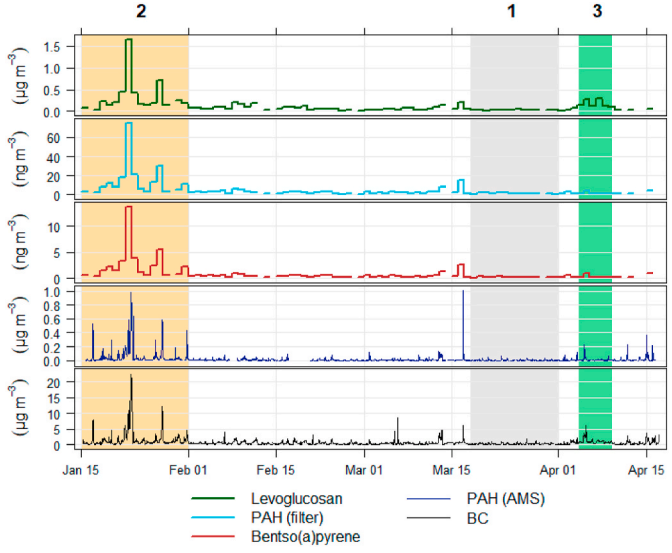

Fig. 2. Time series of biomass burning tracers together with the concentration of BC during the whole measurement campaign. The periods selected for detailed investigation are highlighted by different colours and numbers (2 wood burning = orange, 1 urban background = grey, 3 LRT = green). (For interpretation of the references to colour in this figure legend, the reader is referred to the Web version of this article.)

Time series of the PMF factors calculated from the SP-AMS organics data are shown in Fig. S8. The factors for primary organic aerosol (POA), HOA that is typically connected to motor vehicle emissions and BBOA that is connected to biomass burning, showed the highest concentrations in January. The elevated concentrations of these factors are due to local wood burning together with reduced mixing and dilution of wood burning and traffic related pollutants during the inversion episodes. The mean concentration of SV-OOA did not show large variations between the months, although it showed some high concentrations in January resembling the time series of BBOA (Fig. S8) and an increase in its mean concentration in April. The concentration of the most oxidized organic factor LV-OOA-LRT was highest in April, and it was connected to a strong LRT episode. Also the concentrations of secondary inorganics were high during the LRT episode, but mostly they coincidence with LV-OOA indicating a common origin (Figs. S6 and S8). LV-OOA showed increased concentrations frequently during the measurement period. The source of LV-OOA may be either regional or long-range transport of particulate matter to the measurement site.

Mean diurnal variations of the PMF factors are shown in Fig. S9. The two most oxidized organic factors, LV-OOA and LV-OOA-LRT, did not show any clear diurnal cycles, which is quite typical since secondary organic aerosol (SOA) is either regionally distributed or long-range transported to the measurement site in wintertime. Due to the lack of solar radiation in Helsinki in wintertime, the oxidation of precursor gases takes place mostly via nitrate radical reactions in night-time. The diurnal variation of SV-OOA showed an afternoon minimum in its concentrations. The difference between afternoon minimum and night-time maximum increases when moving from winter to spring, which indicates the semi-volatile nature of SV-OAA as the day-to-night temperature difference increases towards spring.

Diurnal variation of POA factors, HOA and BBOA, showed clear diurnal trends. The late evening maximum of BBOA is probably due to wood burning in the afternoon and evenings, and the HOA morning maximum is connected to motor vehicle emissions during the morning rush hour. Elevated late evening HOA concentration may be an indication that also HOA is formed in wood burning process, or that the motor vehicle related HOA is accumulated in the boundary layer in the evening. Similar diurnal variations of HOA and BBOA factors in the detached house in the Helsinki metropolitan area were reported by Aurela et al. (2015) and in an urban background area by Carbone et al. (2014).

3.2. PM sources in residential area

Three different time periods were chosen for more detailed analysis in order to understand the factors affecting air quality at the measurement site. Based on the variations in the measured particle physical parameters, chemical species and meteorology, the subperiods were found to be dominated by urban background, wood burning and long-range transport aerosol. The chosen periods are marked with different colours in Figs. 1 and 2 and the chosen time intervals are summarized in Table 1 together with the mean PM_1, PN, LDSA, NO_x, benzo(a)pyrene, MA, organic and the sum of inorganic ion concentrations. A more detailed characterization of each period is given in sections 3.2.1-3.2.3. Fossil fuel and wood burning BC fractions and the number and LDSA size distributions are discussed separately in sections 3.2. and 3.3.

The chosen periods were:

1.) **Urban background**, representing typical air quality situation at an urban detached house area with no single dominating source. For the urban background, a two-week period at the end of March with a low PM_1 concentration (mean 3.1 $\mu g\ m^{-3}$) was selected.

During the urban background period, no strong long-range transport episodes were observed, and based on the biomass burning tracers from the filter and PMF analysis, the influence of local wood burning was already diminished due to increased ambient temperature and decreased need to heat buildings. Also, according to meteorological and air quality data, no strong inversion situations took place during this period. In terms of traffic, the effect of the nearby street was minimal since it was closed major part of this period.

2.) **Wood burning**, representing air quality when the impact of local wood burning was significant. For the wood burning, a two-week period in January was selected. During that period, temperature was low, which increased domestic wood burning and also caused temperature inversion situations. Elevated concentration of BBOA, PAH and MAs (Table 1) indicated a strong influence of wood burning emissions. Time series of levoglucosan, benzo(a) pyrene and the sum of analysed PAH from the PM_{10} filter samples are shown in Fig. 2 together with the total PAH concentration obtained from the SP-AMS measurements.

3.) **Long-range transport (LRT)**, representing situation when air quality was influenced by long-range transport. A strong LRT episode was observed as a five-day period in the beginning of April (Table 1, Fig. 1). During these days, elevated concentrations of PM_1 and LV-OOA-LRT were measured (Fig. S8). Increased $PM_{2.5}$ concentration was also observed at the regional background station about 20 km from the measurement site indicating that the increase in pollutant concentrations was not local. Air mass back trajectories confirmed that air masses arrived in Helsinki from Eastern Europe.

3.2.1. *Urban background*

Mean PM_1 concentration was the lowest during the period representing urban background aerosol. When strong local or LRT sources are missing, the measurement site was mostly affected by regionally dispersed traffic and biomass combustion related pollutants. The relatively low concentrations of PN, NO_x and BC during the morning rush hours (Fig. S10) indicated that the influence of local traffic was minimal, although they had similar diurnal profiles as during the whole campaign with a clear morning peak. As the urban background period was in March, the mixing height was greater than in wintertime and the additional dilution of relatively low concentrations of traffic related pollutants probably prevented the detection of the afternoon rush hour peak clearly. In contrast to these, BC showed high concentrations in late evening, which indicated that it was not only connected to traffic related emissions but also to residential wood burning. Although the BC concentration from local wood burning in the late evening was small, its contribution to the total BC concentration was larger than the contribution of traffic related morning BC. Wood burning is likely to have some contribution to BC concentrations throughout the year at the measurement site since many of the detached houses are typically equipped with wood-fired sauna stoves which are used around the year. Also, the mass size distribution of rBC (Fig. 3) supported the influence of wood burning emissions as it had a maximum at a rather large particle size (~500 nm), but we note that a large fraction of BC can also be originating from LRT in Helsinki (Niemi et al., 2009; Luoma et al., 2021). Traffic related fresh BC is typically seen at ~100 nm (Enroth et al., 2016). The fraction of BC in PM_1 was 11% (Fig. 4) which was similar to the BC fraction measured in the heavily traffic influenced Helsinki city centre (Teinilä et al., 2019), although the absolute concentration of BC was much less at the detached house measurement site.

The concentrations of the chemical species measured by the SP-AMS were also very low, their sum being on average 2.1 μg m^{-3}. Largest fraction of the analysed mass consisted of organics (61%). In terms of particle size, inorganic species (sulphate, ammonium and nitrate) had a maximum at ~400–600 nm (D_{va}) with the similar mass size distributions suggesting that they all were mostly related to regionally distributed or LRT aerosol (Fig. 4). Organics peaked at slightly smaller size (~350–400 nm) and had a wider mode extending to the small particle size. This indicated organics having also some contribution from local sources e.g., from traffic.

The relative abundances of the different PMF factors are shown in Fig. 4. The fraction of HOA, typically related to traffic, showed a contribution of 12% for the urban background period, although its absolute concentration was very low (Fig. S8). The percentages of the other PMF factors indicate that, in addition to traffic related pollutants, the site was also affected at some degree by wood burning (9%) and LRT aerosol (32%) during the urban background period (Fig. 4). Elevated concentrations of total PAH (measured with the SP-AMS) were also seen at the late evening (Fig. S10), however, the mean concentrations of benzo(a)pyrene and PAH (PM_{10} filter samples and SP-AMS) were much lower during the urban background period than during the wood burning period (Table 1, Fig. 1 and Fig. S11). The lack of strong inversion situations also prevented pollutants to accumulate on the boundary layer in March.

3.2.2. *Wood burning*

Markedly elevated PM_1 concentrations together with the campaign-highest BC concentrations were measured during the two-week period on January 15–31, 2019, which was selected as a wood burning period (Table 1, Fig. 1). BBOA, levoglucosan, PAH (PM_{10} filter samples and SP-AMS) and benzo(a)pyrene all showed the highest mean concentrations during the wood burning period (Fig. 2 and Fig. S8). The concentration of levoglucosan was elevated also in April during the LRT period, but the concentration of benzo(a)pyrene and PAH measured with the SP-AMS did not increase in April indicating that the latter ones are more specific tracers for local wood burning. Also in an earlier study, residential wood combustion was found to be the main source of benzo(a)pyrene in Helsinki Metropolitan area (Hellén et al., 2017). The two days with the highest concentrations of BC and wood burning tracers (Jan. 22 and Jan. 28) were also the coldest days during the measurement period showing temperatures below −20 °C and below −15 °C correspondingly.

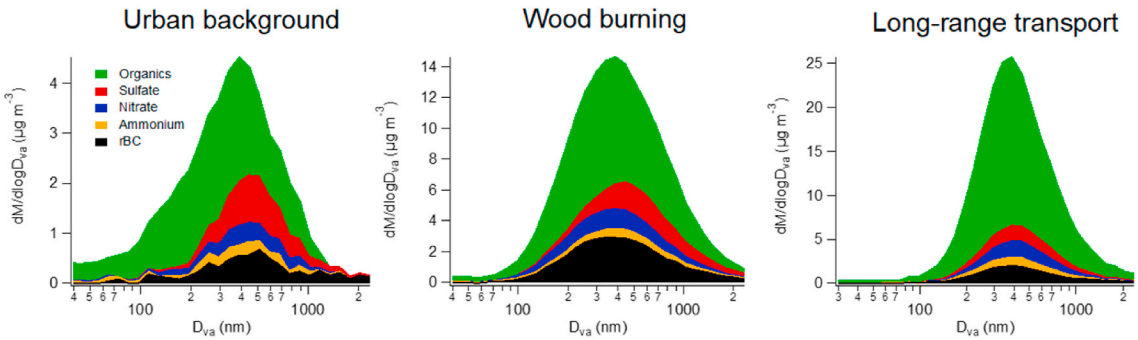

Fig. 3. Mean mass size distributions for the major chemical components during urban background, wood burning and LRT periods.

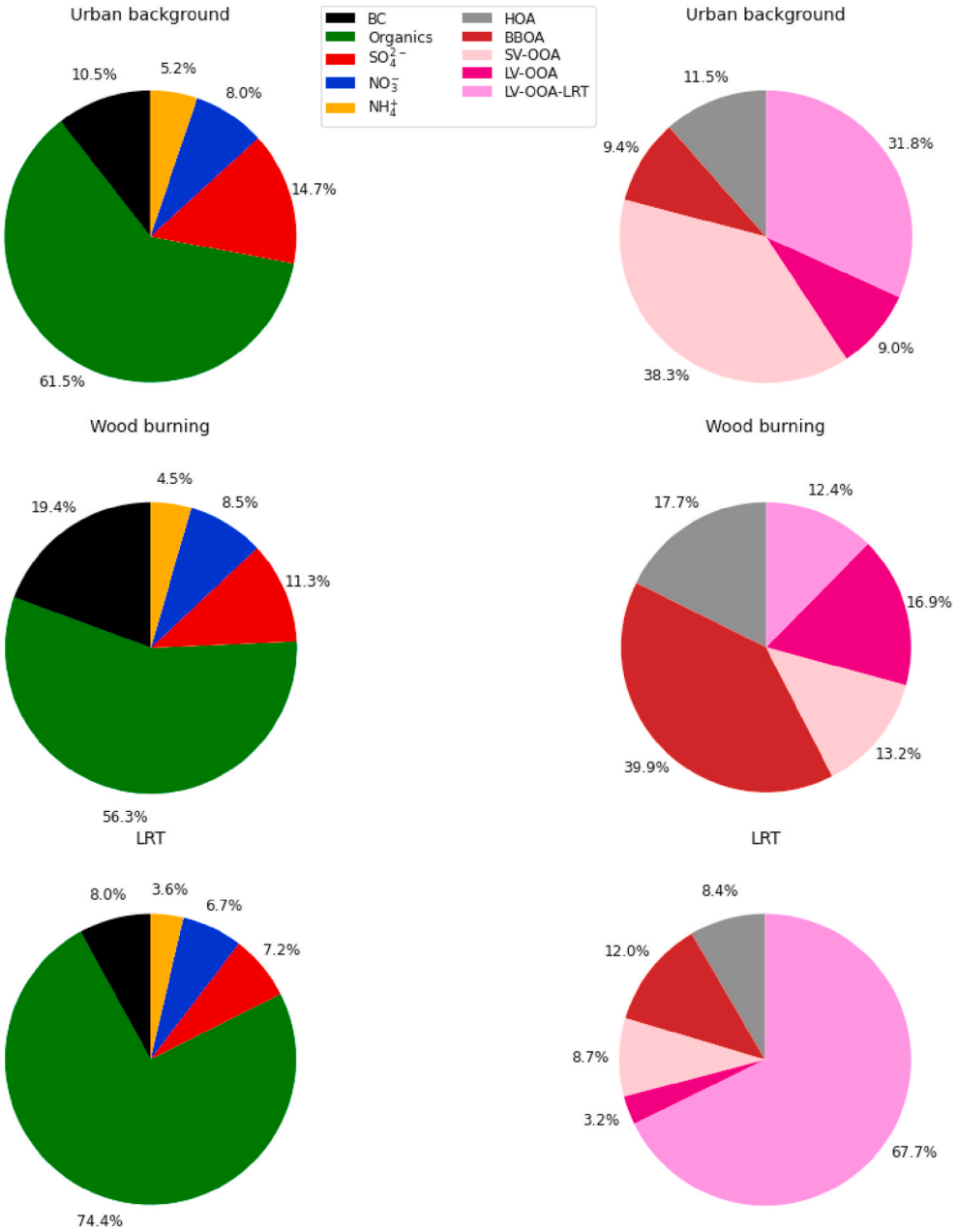

Fig. 4. Mass fractions of the measured major chemical components and PMF factors for organics during urban background, wood burning and LRT dominated periods.

During the wood burning period, the relative contribution of BC to PM_1 was clearly higher compared to its contribution during the urban background period (Fig. 4). BC had two daily maxima during the wood burning period (Fig. S11) of which the evening peak was clearly higher for BC. Additionally, the morning maximum BC peaked later than the maximum during the urban background period suggesting that also BC in the morning could be partly related to wood burning since the morning peak can be seen also in the concentrations of other wood burning tracers PAH and BBOA. However, the evening peak was clearly larger also for the PAH and BBOA than the morning peak (Fig. S11). The evening maximum for NO_x and HOA (Fig. S11) indicated that wood burning may also be the origin for these compounds, or that motor vehicle related pollutants are trapped and accumulated in the boundary layer during cold periods with minimal dilution and mixing of pollutants.

During the wood burning period chloride showed its campaign-highest mean concentration (0.06 μg m^{-3}), and its maximum values were detected between 12–23 p.m. (not shown). Chloride can be either emitted from wood burning or it has accumulated in the boundary layer from the other sources due to low mixing of pollutants. Regarding the size distributions, organics and rBC had very similar mass size distributions peaking at ~350 nm particle size (Fig. 3). Nitrate and ammonium had a maximum at larger particle size (at ~400 nm) indicating them to be related to other sources than biomass combustion or having different atmospheric processing from organics and BC. Sulphate peaked at the largest size (~450 nm).

3.2.3. *Long-range transport*

Period with a strong long-range transport of particulate matter took place between 4 and 9 April 2019. Of three chosen periods, the highest mean PM_1 concentration was measured during the LRT period (14.6 μg m^{-3}, Table 1). On average, 74% of the measured PM_1 chemical

components consisted of organics its mean concentration being 9.9 μg m^{-3} during the LRT period. The largest fraction of organics was composed of the most oxidized organic factor LV-OOA-LRT (Fig. 4). The concentrations of the secondary inorganic aerosol components, sulphate, nitrate and ammonium, were also elevated (Fig. S6).

Relatively high concentrations of BBOA (Fig. S8) and levoglucosan (Fig. 2) together with the elevated concentration of organics indicated that the LRT aerosol contained also biomass burning originated material. According to the NAAPS model results (not shown) and calculated air mass back trajectories (Fig. S12), smoke aerosol arrived in Helsinki from open fires in Eastern Europe. Elevated concentration of submicron particles, containing aged organic material and MAs originated from burning of agricultural waste of previous season, has been measured in Helsinki during springtime also in the earlier studies (Saarnio et al., 2010a,b; Saarikoski et al., 2007). As mentioned earlier, the concentration of benzo(a)pyrene and concentration of PAH obtained from the SP-AMS measurements did not show clear increase during the LRT period. The degradation and lifetime of PAHs will be discussed in section 3.4.

The concentration of BC was also elevated during the LRT period (Table 1, Fig. 1), and its origin is most likely LRT biomass burning, but it may also partly explain by traffic related emission. All motor vehicle emission indicators, BC, NO_x, HOA and PN, showed a clear morning peak during the LRT period (Fig. S13), and the increase in their concentrations in the morning was much larger than during urban background or wood burning periods indicating a strong influence of local or regional traffic related pollutants. However, their concentration throughout the day was also clearly higher, which may indicate that they were also partly long-range transported to the measurement site. In terms of size-distributions, all chemical species had a maximum at ~400–450 nm except rBC that peaked at slightly smaller size at ~350–400 nm. This also supports the finding that BC originated partly from traffic emissions, whereas the other species were mostly internally mixed during the transport.

3.3. Fossil fuel and wood burning BC fractions

The diurnal variations of fossil fuel (BC_{ff}) and wood burning (BC_{wb}) fractions of BC during the three periods are shown in Fig. S14. When comparing the periods, it was found that during the urban background period the contribution of BC_{ff} was larger (mean 76% of BC) than that of BC_{wb}, whereas during the wood burning and LRT periods the contribution of BC_{wb} was higher (mean 68 and 78% of BC, respectively). The largest difference in the diurnal trends of BC_{ff} and BC_{wb} was found during the urban background period, where the morning BC_{ff} peak is clearly larger compared to the BC_{wb} peak. The evening peak can be found for both BC_{ff} and BC_{wb} during the urban background and wood burning periods. Also, the PMF analysis attributed both BBOA and HOA to late evenings similar to BC_{ff} and BC_{wb}. This seems to be due to the mixing of local wood burning and traffic related particulate matter in the evening, but one possibility is also that wood burning aerosol contain also BC_{ff} and HOA type organic aerosol. However, in general, this indicates that, when measuring wood burning aerosol in the vicinity of other emission sources, the interpretation of the results is not so straightforward.

3.4. Particle number and LDSA size distributions

The mean particle number size distributions for the selected three periods are shown in Fig. 5. Number size distributions differed notably between the periods. During the urban background period, the number size distribution had two modes both at the size range between 10 and 50 nm. Compared to the urban background period, the particle number size distribution was clearly shifted to the larger particle size during the wood burning period when the size distribution was unimodal with the maximum at ~30–40 nm. Also, the total particle number concentration was higher during the wood burning period (Fig. 5, Table 1). During the LRT period, the mode at 10–20 nm was roughly similar to that during the urban background period, however, a mode in the particle size larger than 0.1 μm was also observed. This second mode is most likely connected to the aged aerosol formed by the accumulation of secondary organic and inorganic matter on particles during transport.

LDSA concentration is directly connected to particle size distribution and concentration. In this study, the highest mean LDSA concentration measured by the AQ™ Urban instrument was detected during the LRT period (18.2 μm^2 cm^{-3}, Table 1) followed closely by the wood burning period (16.2 μm^2 cm^{-3}). During the urban background period the LDSA concentration was much smaller (6.0 μm^2 cm^{-3}). Mean LDSA size distributions calculated from the SMPS data are shown in Fig. 5. It is evident that during the LRT period the LDSA size distribution had a maximum at clearly larger particle size than during the urban background and wood burning periods. Similar results have been published by Salo et al. (2021) who found out that the maximum of the LDSA size distribution was at larger particle size during the LRT episode than during the influence of local sources measured at the street canyon site in Helsinki. However, the LDSA particle size was even larger in Delhi, India. In terms of the diurnal variations, the LDSA concentrations during the three selected periods (urban background, wood burning and LRT,

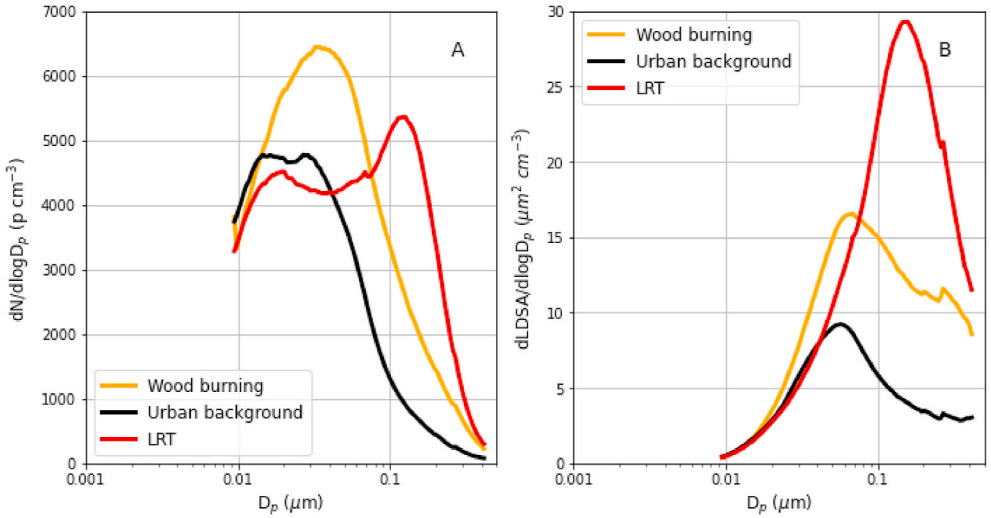

Fig. 5. Ambient particle number (A) and LDSA (B) size distributions measured with the SMPS during different periods (Wood burning, Urban background, LRT).

Fig. S15) showed both morning and late evening peaks, responding both to traffic and wood burning related pollutants.

3.5. Comparison of different metrics for different periods

The mean and median concentrations of PM_1, LDSA, PN, BC, NO_x and benzo(a)pyrene during urban background, wood burning, and LRT period are shown in Fig. 6. The concentrations of all those species were smallest during the urban background period (Table 1, Fig. 6). This is expected since the urban background period was chosen so that it represents the time period of no strong effect of local or long-range transported pollutants. The mean concentration of PN did not show very large variations between the periods, although its highest mean concentration was measured during the wood burning period, but also the variation was largest during that period. It is possible that PN originated mostly from a local source like traffic, and partly from wood burning, but especially traffic related sources were present throughout the measurement period.

The mean concentrations of NO_x, BC and benzo(a)pyrene were highest during the wood burning period. The increase was most significant to benzo(a)pyrene that had roughly ten times larger mean concentration during the wood burning period compared to the urban background period. In air quality point of view, this is highly important due to carcinogenic nature of benzo(a)pyrene and other PAHs. In addition to local wood burning, also the accumulation of traffic related pollutants impaired air quality during the cold and calm wood burning period.

LRT affected greatest the PM_1 and BC concentrations that were 4.7 and 3.7 larger during the LRT period compared to the urban background period, respectively. The high PM_1 concentration during the LRT episode is probably due to the accumulation of secondary organic and inorganic species on primary particles during the transport increasing particle size and total mass. Also LSDA and NO_x concentrations were affected by the LRT shown by roughly three times larger concentrations during the LRT period than the urban background period. During the LRT period, particles originated at least partly from open fires, but benzo (a)pyrene and other PAH concentrations were not elevated during the LRT period. It is possible that they may have been lost before arriving in Helsinki due to their short atmospheric lifetimes (Ravindra et al., 2008) that are highly dependent on particle type and the viscosity of SOA coating of the particles. Oxidation flow reactor studies have shown that concentration of benzo(a)pyrene decreases with increasing photochemical age (Miersch et al., 2019) so it is possible that benzo(a) pyrene had degraded during the transport. In general, the lifetime of benzo(a) pyrene has been estimated to vary from minutes up to 5 days (Shrivastava et al., 2017, Shimada et al., 2020). Therefore, the results in our study indicate that benzo(a)pyrene is merely an indicator of local wood burning and not long-range transported biomass burning emissions. In contrast to benzo(a)pyrene, LRT affected notably MA concentration with seven times larger concentration during the LRT period compared to the urban background period (Table 1). It should be noted that also the levoglucosan has been shown to be prone to hydroxyl radical exposure (Hennigan et al., 2010), and the atmospheric lifetimes of levoglucosan have been estimated to be 1.2–3.9 days under different conditions (Lai et al., 2014). Besides different atmospheric lifetimes, another possibility for different benzo(a)pyrene-to-levoglucosan ratio for local and LRT biomass combustion particles is that the production yields of benzo(a) pyrene and levoglucosan are different in controlled wood burning and open fire situations. However, that is less likely explanation.

Fig. 7 shows the correlation between the LDSA concentrations and PM_1, PN and BC concentrations in order to examine if the measurements of ambient PM_1, PN and/or BC could be used to estimate the LDSA

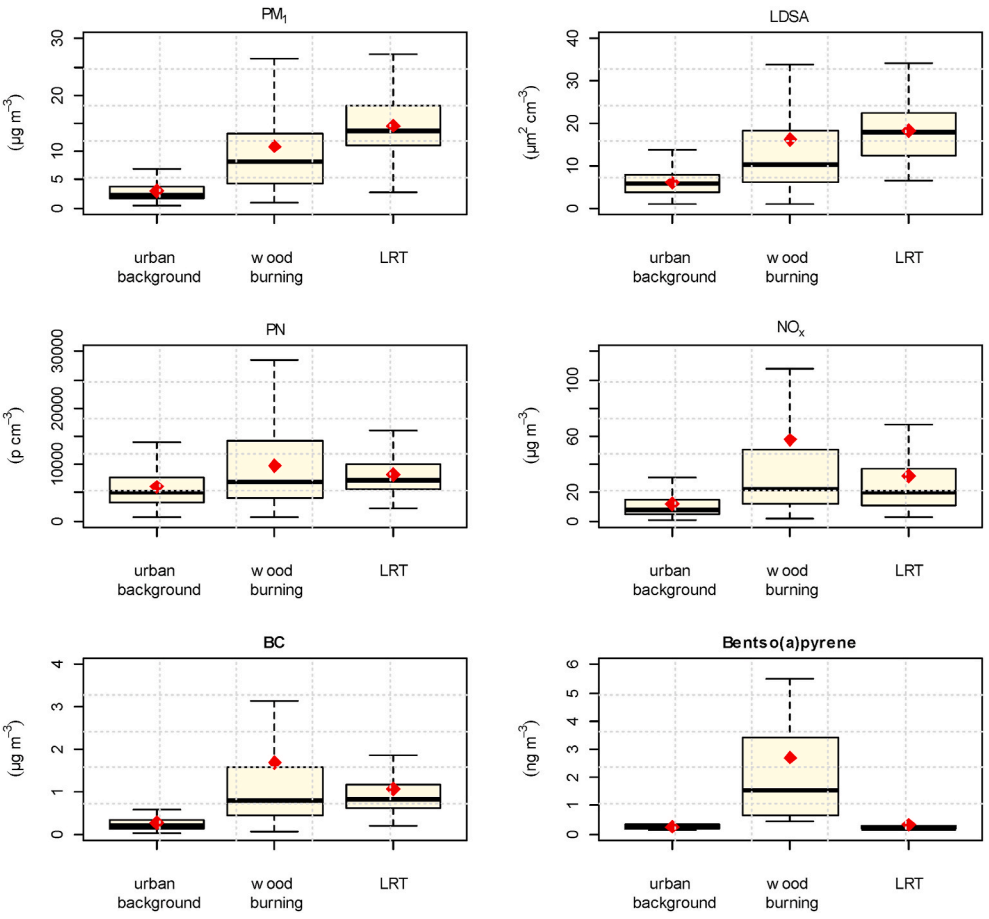

Fig. 6. Boxplots of PM_1, LDSA, PN, NO_x, BC and benzo(a)pyrene concentrations during the three selected periods (urban background, wood burning and LRT). Boxplot shows the median concentrations (line in the middle of box) together with minimum (lower line), maximum (upper line), and 25th (bottom of box) and 75th (top of box) percentiles. Outliers are not shown. The mean concentration is shown with red squares. (For interpretation of the references to colour in this figure legend, the reader is referred to the Web version of this article.)

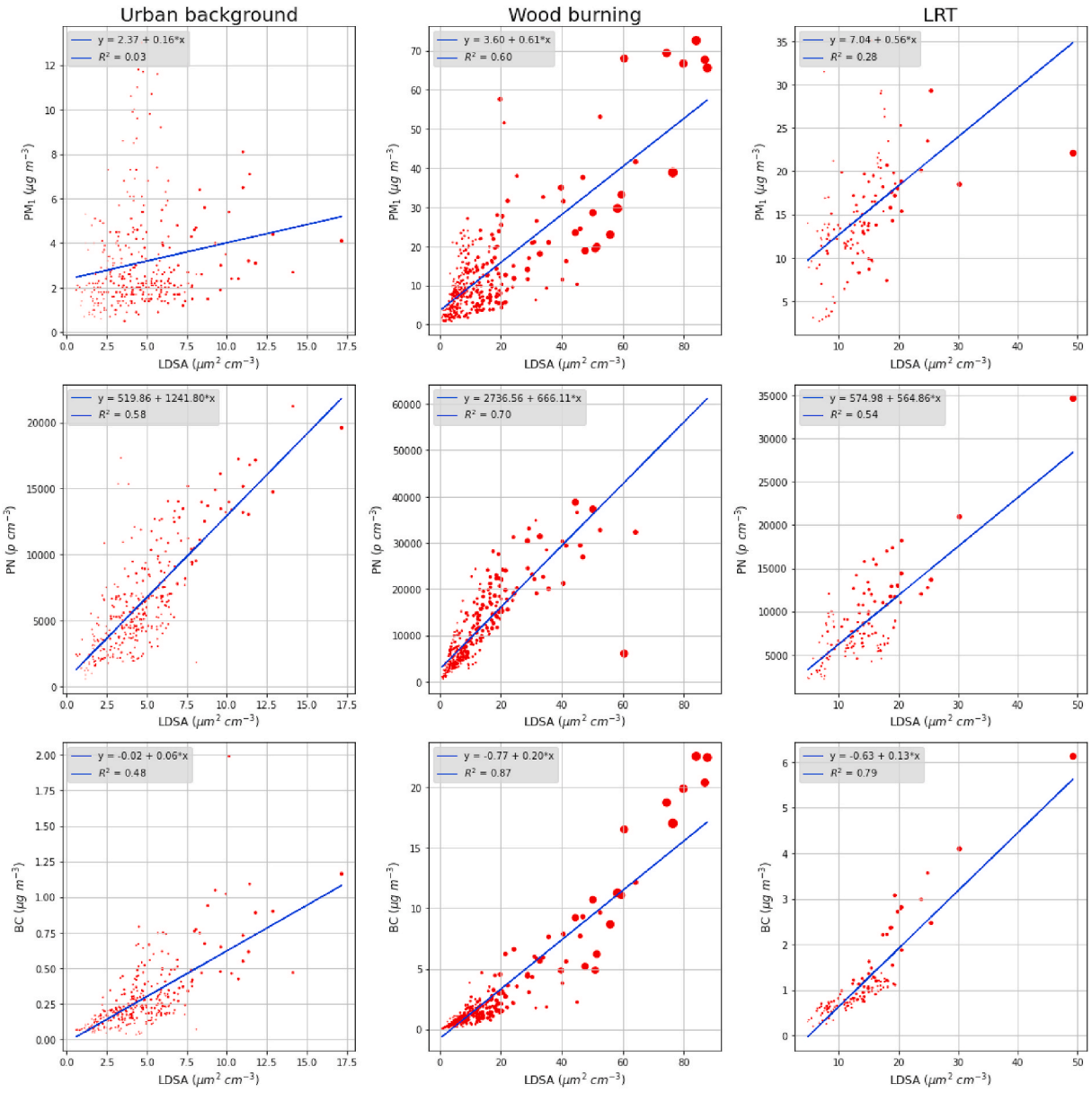

Fig. 7. Correlation between LDSA and PM_1, PN and BC during the three selected periods (urban background, wood burning and LRT). The size of the marker is proportional to the measured NO_x concentration at the same hour.

loading during different periods. For the urban background period, there was a correlation between the LDSA concentration and PN and BC concentrations, although the R^2 values were not very high ($R^2 = 0.54$ and $R^2 = 0.50$, respectively). PM_1 concentration did not correlate with the LDSA concentration during the urban background period. The correlation between LDSA and PN and BC concentrations during the urban background period is probably connected to soot particle and nucleation modes which originate typically from motor vehicle exhausts. During the wood burning period, the PN and BC concentrations showed high correlations with the LDSA concentration, R^2 being 0.87 for BC and 0.78 for PN. The correlation between the PM_1 and LDSA concentration was also higher being 0.52. The high correspondence between the BC and LDSA concentrations indicated that the BC particles increase also the LDSA concentration. These may be either wood burning originated soot particles or traffic related soot particles near 100 nm accumulated in the boundary layer, however, based on the mass size distributions from the SP-AMS (Fig. 3), there was no clear mode at ~100 nm for BC during the wood burning period. The correlation between LDSA and BC fractions, BC_{ff} and BC_{wb}, were nearly similar during the urban background and wood burning periods, but a larger difference was found during the LRT period. During the LRT period, the correlation coefficient (R^2) between LDSA and BC_{ff} was 0.59, and between LDSA and BC_{wb} 0.83. This further confirms that the calculated BC_{wb} fraction of BC is more selectively connected to aged biomass burning originated BC. The moderate correlation between PM_1 and LDSA concentrations also indicate that particles were larger in their size during this period, which was also seen from the LDSA particle size distributions. During the LRT period, the correlation coefficients between BC, PN and PM_1 concentrations and LDSA concentration were 0.79, 0.55 and 0.27 respectively.

According to the measurement results presented in this study, the LDSA concentration seem to follow the BC concentration in all three cases, i.e., in cases of urban background period, wood burning, and LRT aerosol dominated periods. The second-highest correlations were found between PN and LDSA concentrations. Lowest correlation was found between PM_1 and LDSA concentrations. Poor correlation between $PM_{2.5}$ and LDSA concentrations at urban background and residential detached

house sites in Helsinki has also been reported by Kuula et al. (2020b) and Kuuluvainen et al. (2016).

4. Conclusions

In this study, the sources affecting air quality in an urban detached housing area in Helsinki were identified and characterized. Special attention was paid on the parameters that can be utilized to estimate the main particle sources and to assess their impact on air quality. Three periods were chosen for the detailed investigation based on the differences in particle physical and chemical properties and meteorology. The PMF factors obtained from the SP-AMS were also used to select the periods. During the investigated periods, the ambient particulate matter was dominated by urban background, wood burning and long-range transported aerosols.

According to our measurements, different particle metrics emphasize different particles sources. Particle number concentration was a good indicator of local combustion, especially traffic emissions. PN showed a clear increase during the morning rush hour in all three periods being a good indicator for traffic emissions. However, the afternoon traffic hour was seen only as a slight increase during the urban background and wood burning periods likely due to the more efficient mixing of emissions as well as less clear traffic accumulation. When comparing the mean PN concentrations during different periods, PN concentration was relatively stable, although a slight increase in mean PN concentration was observed during the wood burning period. The increase in PN concentrations during the wood burning period was probably connected both to local wood burning and the accumulation of traffic related pollutants on the boundary layer.

BC was influenced by both motor vehicle emissions and wood burning evidenced by the morning peak during traffic hour and late evening peak in cold months. In terms of different periods, the largest mean BC concentration was observed during the wood burning period followed by the LRT period. Moreover, during the wood burning and LRT periods, the contribution of BC related to wood burning (BC_{wb}) was higher than that related to fossil fuel combustion (BC_{ff}), whereas during the urban background period BC_{ff} dominated BC throughout the day. The evening peak was found for both BC_{ff} and BC_{wb} during the urban background and wood burning periods, which seemed to be related to the mixing of local wood burning and traffic related particulate matter in the evening, but it is also possible that wood burning aerosol contained BC_{ff}. However, in general this shows that, when measuring wood burning aerosol in the vicinity of other emission sources, the interpretation of the results can be challenging.

Increased concentrations of PAHs and MAs were connected to the biomass burning emissions. The increase was most significant to benzo (a)pyrene and MAs that had ten times larger mean concentrations during the wood burning period compared to the urban background period. Benzo(a)pyrene and PAH were predominantly connected to the local wood burning events as they did not show marked increase during the LRT period, although during the LRT period particles originated at least partly from open fires evidenced by seven times larger concentration of MAs during the LRT period compared to the urban background period. In addition to PAHs being good indicators of wood combustion, much higher relative contribution of benzo(a)pyrene and other PAHs during the wood combustion periods is very significant due to the carcinogenic nature of these compounds. This also indicates that particulate matter originating from local wood combustion may be even more harmful than expected just based on the PM levels.

The LDSA concentration followed the BC concentration during all three periods even though the main particle source was different. After BC, the next strongest correlation was found between PN and LDSA concentrations, especially during the wood burning period. The lowest correlation was found between PM_1 and LDSA concentrations. The diurnal variation of LDSA during different periods showed that the LDSA concentration responded to the elevated traffic related emissions in the morning and local wood burning emissions in the late evening. The largest mean LDSA concentrations were, however, detected during the LRT period together with the LDSA size distribution located at the largest particle size.

Elevated PM_1 concentration was attributed especially to the periods containing particles with larger particle size, such as LRT and local wood burning in fireplaces. During the LRT episode, the PM_1 concentration was five times larger compared to the urban background period. PM_1 together with secondary organic and inorganic particulate species were good indicators of strong LRT episodes.

In conclusion, monitoring of non-regulated particle parameters (e.g., BC, LDSA, PN) increases understanding on the properties and sources of fine particles, especially related to the emissions from local combustion. The use of high-time resolution instruments allows to explore the diurnal variation of pollutants and provides valuable information on rapidly changing pollutant concentrations that are characteristics for local sources. However, none of the investigated single parameters describes the source or health effect of particles solely, which emphasizes the utilization of a set of monitoring devices.

CRediT authorship contribution statement

K. Teinilä: Writing – original draft, Formal analysis, Visualization, Data curation. **H. Timonen:** Project administration, Writing – original draft, Supervision. **M. Aurela:** Investigation, Writing – review & editing, Formal analysis. **J. Kuula:** Investigation, Writing – review & editing, Formal analysis. **T. Rönkkö:** Project administration, Funding acquisition, Writing – review & editing, Conceptualization. **H. Hellèn:** Investigation, Formal analysis, Writing – review & editing. **K. Loukkola:** Investigation, Formal analysis, Writing – review & editing. **A. Kousa:** Investigation, Formal analysis, Writing – review & editing. **J.V. Niemi:** Project administration, Writing – original draft, Conceptualization. **S. Saarikoski:** Project administration, Funding acquisition, Writing – original draft, Conceptualization, Supervision.

Declaration of competing interest

The authors declare that they have no known competing financial interests or personal relationships that could have appeared to influence the work reported in this paper.

Acknowledgments

Long-term research co-operation and support from HSY to this project is gratefully acknowledged. Financial support from Black Carbon Footprint project funded by Business Finland and participating companies (Grant 528/31/2019), from European Regional Development Fund, Urban innovative actions initiative (HOPE; Healthy Outdoor Premises for Everyone, project nro: UIA03-240), from MegaSense Growth Engine: Air Quality Monitoring funded by Business Finland (Grant 7517/31/2018) and Academy of Finland Flagship ACCC (grant no. 337552, 337551) are gratefully acknowledged.

Appendix A. Supplementary data

Supplementary data to this article can be found online at https://doi.org/10.1016/j.atmosenv.2022.118939.

References

Alfarra, M.R., Prevot, A.S.H., Szidat, S., Sandradewi, J., Weimer, S., Lanz, V.A., Schreiber, D., Mohr, M., Baltensperger, U., 2007. Identification of the mass spectral signature of organic aerosols from wood burning emissions. Environ. Sci. Technol. 41, 5770–5777.

Atkinson, R.W., Kang, S., Anderson, H.R., Mills, I.C., Walton, H.A., 2014. Epidemiological time series studies of PM2.5 and daily mortality and hospital admissions: a systematic review and meta-analysis. Thorax 69, 660–665, 2014.

Aurela, M., Saarikoski, S., Niemi, J.V., Canonaco, F., Prevot, A.S.H., Frey, A., Carbone, S., Kousa, A., Hillamo, R., 2015. Chemical and source characterization of submicron particles at residential and traffic sites in the Helsinki metropolitan area, Finland. Aerosol Air Qual. Res. 15 (4), 1213–1226. https://doi.org/10.4209/aaqr.2014.11.0279.

Barreira, L.M.F., Helin, A., Aurela, M., Teinilä, K., Friman, M., Kangas, L., Niemi, J.V., Portin, H., Kousa, A., Pirjola, L., Rönkkö, T., Saarikoski, S., Timonen, H., 2021. In-depth characterization of submicron particulate matter inter-annual variations at a street canyon site in Northern Europe, Atmos. Chem. Phys. 21, 6297–6314. https://doi.org/10.5194/acp-21-6297-2021.

Brown, D.M., Wilson, M.R., MacNee, W., Stone, V., Donaldson, K., 2001. Size-dependent proinflammatory effects of ultrafine polystyrene particles: a role for surface area and oxidative stress in the enhanced activity of ultrafines. Toxicol. Appl. Pharmacol. 175 (3), 191–199. https://doi.org/10.1006/taap.2001.9240.

Canagaratna, M.R., Jayne, J.T., Ghertner, D.A., Herndon, S., Shi, Q., Jimenez, J.L., Silva, P.J., Williams, P., Lanni, T., Drewnick, F., Demerjian, K.L., Kolb, C.E., Worsnop, D.R., 2004. Chase studies of particulate emissions from in-use New York city vehicles. Aerosol. Sci. Technol. 38, 555–573.

Carbone, S., Aurela, M., Saarnio, K., Saarikoski, S., Timonen, H., Frey, A., Sueper, D., Ulbrich, I.M., Jiminez, J.L., Kulmala, M., Worsnop, D.R., Hillamo, R.E., 2014. Wintertime aerosol chemistry in sub-arctic urban air. Aerosol Sci. Technol. 48, 313–323.

Carbone, S., Saarikoski, S., Frey, A., Reyes, F., Reyes, P., Castillo, M., Gramsch, E., Oyola, P., Jayne, J., Worsnop, D., Hillamo, R., 2013. Chemical Characterization of Submicron Aerosol Particles in Santiago de Chile. Aerosol Air Qual. Res. 13, 462–473.

Carslaw, D.C., Ropkins, K., 2012. Openair–an R package for air quality data analysis. Environ. Model. Software 27–28, 52–61.

Drinovec, L., Močnik, G., Zotter, P., Prévôt, A., Ruckstuhl, C., Coz, E., Rupakheti, M., Sciare, J., Müller, T., Wiedensohler, A., 2015. The" dual-spot" Aethalometer: an improved measurement of aerosol black carbon with real-time loading compensation. Atmos. Meas. Tech. 8, 1965–1979.

Dzepina, K., Arey, J., Marr, L.C., Worsnop, D.R., Salcedo, D., Zhang, Q., Onasch, T.B., Molina, L.T., Molina, M.J., Jose, L., Jimenez, J.L., 2007. Detection of particle-phase polycyclic aromatic hydrocarbons in Mexico City using an aerosol mass spectrometer. Int. J. Mass Spectrom. 263, 152–170. https://doi.org/10.1016/j.ijms.2007.01.010.

Enroth, J., Saarikoski, S., Niemi, J.V., Kousa, A., Ježek, I., Močnik, G., Carbone, S., Kuuluvainen, H., Rönkkö, T., Hillamo, R., Pirjola, L., 2016. Chemical and physical characterization of traffic particles in four different highway environments in the Helsinki metropolitan area. Atmos. Chem. Phys. 16, 5497–5512.

EU, 2015. DIRECTIVE 2004/107/EC of the EUROPEAN PARLIAMENT and of the COUNCIL of 15 December 2004 Relating to Arsenic, Cadmium, Mercury, Nickel and Polycyclic Aromatic Hydrocarbons in Ambient Air - Amended by Regulation (EC) No 219/2009 of the European Parliament and of the Council of 11 March 2009 and Commission Directive (EU) 2015/1480 of 28 August.

Finnish Transport Infrastructure Agency, 2019. https://julkinen.vayla.fi/webgis-sovellukset/webgis/template.html?config=liikenne.

Gani, S., Bhandari, S., Seraj, S., Wang, D.S., Patel, K., Soni, P., Arub, Z., Habib, G., Hildebrandt Ruiz, L., Apte, J.S., 2019. Submicron aerosol composition in the world's most polluted megacity: the Delhi Aerosol Supersite study. Atmos. Chem. Phys. 19, 6843–6859. https://doi.org/10.5194/acp-19-6843-2019.

Guerreiro, C., Horalek, J., de Leeuw, F., Couvidat, F., 2015. Mapping Ambient Concentrations of Benzo(a)pyrene in Europe – Population Exposure and Health Effects for 2012. ETC/ACM Technical Paper 2014/6.

Hansen, A., Rosen, H., Novakov, T., 1984. The aethalometer–an instrument for the realtime measurement of optical absorption by aerosol particles. Sci. Total Environ. 36, 191–196.

Helin, A., Niemi, J., Virkkula, A., Pirjola, L., Teinilä, K., Backman, J., Aurela, M., Saarikoski, S., Rönkkö, T., Asmi, E., Timonen, H., 2018. Characteristics and source apportionment of black carbon in the Helsinki metropolitan area. Finland Atmos Environ. 190, 87–98. https://doi.org/10.1016/j.atmosenv.2018.07.022.

Hellén, H., Kangas, L., Kousa, A., Vestenius, M., Teinilä, K., Karppinen, A., Kukkonen, J., Niemi, J.V., 2017. Evaluation of the impact of wood combustion on benzo[a]pyrene (BaP) concentrations; ambient measurements and dispersion modeling in Helsinki, Finland. Atmos. Chem. Phys. 17, 3475–3487. https://doi.org/10.5194/acp-17-3475-2017.

Hennigan, C.J., Sullivan, A.P., Collett Jr., J.L., Robinson, A., 2010. Levoglucosan stability in biomass burning particles exposed to hydroxyl radicals. Geophys. Res. Lett. 37, L09806. https://doi.org/10.1029/2010GL043088, 2010.

ICRP, 1994. Human respiratory tract model for radiological protection. A report of a task group of the international commission on radiological protection. Ann. ICRP 24 (1–3), 1–482.

Jansen, R.C., Shi, Y., Chen, J., et al., 2014. Using hourly measurements to explore the role of secondary inorganic aerosol in $PM_{2.5}$ during haze and fog in Hangzhou, China. Adv. Atmos. Sci. 31, 1427–1434. https://doi.org/10.1007/s00376-014-4042-2.

Järvi, L., Junninen, H., Karppinen, A., Hillamo, R., Virkkula, A., Mäkelä, T., Pakkanen, T., Kulmala, M., 2008. Temporal variations in black carbon concentrations with different timescales in Helsinki during 1996–2005. Atmos. Chem. Phys. 8, 1017–1027.

Karjalainen, P., Timonen, H., Saukko, E., Kuuluvainen, H., Saarikoski, S., Aakko-Saksa, P., Murtonen, T., Bloss, M., Dal Maso, M., Simonen, P., et al., 2016. Time-resolved characterization of primary particle emissions and secondary particle formation from a modern gasoline passenger car. Atmos. Chem. Phys. 16 (13), 8559–8570. https://doi.org/10.5194/acp16-8559-2016.

Kupiainen, K., Ritola, R., Stojiljkovic, A., Pirjola, L., Malinen, A., Niemi, J., 2016. Contribution of mineral dust sources to street side ambient and suspension PM10 samples. Atmos. Environ. 147, 178–189.

Kuula, J., Friman, M., Helin, A., Niemi, J.V., Aurela, M., Timonen, H., Saarikoski, S., 2020a. Utilization of scattering and absorption-based particulate matter sensors in the environment impacted by residential wood combustion. J. Aerosol Sci. 150 https://doi.org/10.1016/j.jaerosci.2020.105671.

Kuula, J., Kuuluvainen, H., Niemi, J.V., Saukko, E., Portin, H., Kousa, A., Aurela, M., Rönkkö, T., Timonen, H., 2020b. Long-term sensor measurements of lung deposited surface area of particulate matter emitted from local vehicular and residential wood combustion sources. Aerosol. Sci. Technol. 54 (2), 190–202. https://doi.org/10.1080/02786826.2019.1668909.

Kuuluvainen, H., Rönkkö, T., Järvinen, A., Saari, S., Karjalainen, P., Lähde, T., Pirjola, L., Niemi, J.V., Hillamo, R., Keskinen, J., 2016. Lung deposited surface area size distributions of particulate matter in different urban areas, 2016. Atmos. Environ. 136, 105–113. https://doi.org/10.1016/j.atmosenv.2016.04.019.

Lai, C., Liu, Y., Ma, J., Ma, Q., He, H., 2014. Degradation kinetics of levoglucosan initiated by hydroxyl radical under different environmental conditions. Atmos. Environ. 91, 32–39. https://doi.org/10.1016/j.atmosenv.2014.03.054.

Lammel, G., 2015. Polycyclic aromatic compounds in the atmosphere – a review identifying research needs. Polycycl. Aromat. Comp. 35 (2–4), 316–329. https://doi.org/10.1080/10406638.2014.931870.

Leino, K., Riuttanen, L., Nieminen, T., Dal Maso, M., Väänänen, R., Pohja, T., Keronen, P., Järvi, L., Aalto, P.P., Virkkula, A., Kerminen, V.-M., Petäjä, T., Kulmala, M., 2014. Biomass burning smoke episodes in Finland from Russian wildfires. Boreal Environ. Res. 19 (B), 275–292.

Lelieveld, J., Evans, J.S., Fnais, M., Giannadaki, D., Pozzer, A., 2015. The contribution of outdoor air pollution sources to premature mortality on a global scale. Nature 525 (7569), 367–371. https://doi.org/10.1038/nature15371.

Luben, T.J., Nichols, J.L., Dutton, S.J., Kirrane, E., Owens, E.O., Datko-Williams, L., Madden, M., Sacks, J.D., 2017. A systematic review of cardiovascular emergency department visits, hospital admissions and mortality associated with ambient black carbon. Environ. Int. 107, 154–162. https://doi.org/10.1016/j.envint.2017.07.005.

Luoma, K., Niemi, J.V., Aurela, M., Fung, P.L., Helin, A., Hussein, T., Kangas, L., Kousa, A., Rönkkö, T., Timonen, H., Virkkula, A., Petäjä, T., 2021. Spatiotemporal variation and trends in equivalent black carbon in the Helsinki metropolitan area in Finland. Atmos. Chem. Phys. 21, 1173–1189. https://doi.org/10.5194/acp-21-1173-2021, 2021.

Magee Scientific, 2016. Aethalometer® Model AE33 User Manual Version 1.54. Magee Scientific.

Miersch, T., Czechb, H., Hartikainen, A., Ihalainen, M., Orasche, J., Abbaszade, G., Tissari, J., Streibela, T., Jokiniemi, J., Sippula, O., Zimmermann, R., 2019. Impact of photochemical ageing on Polycyclic Aromatic Hydrocarbons (PAH) and oxygenated PAH (Oxy-PAH/OH-PAH) in logwood stove emissions. Atmos. Environ. 686, 382–392. https://doi.org/10.1016/j.scitotenv.2019.05.412.

Niemi, J.V., Saarikoski, S., Aurela, M., Tervahattu, H., Hillamo, R., Westphal, D.L., Aarnio, P., Koskentalo, T., Makkonen, U., Vehkamäki, H., Kulmala, M., 2009. Long-range transport episodes of fine particles in southern Finland during 1999–2007. Atmos. Environ. 43, 1255–1264.

Niemi, J.V., Tervahattu, H., Vehkamäki, H., Kulmala, M., Koskentalo, T., Sillanpää, M., Rantamäki, M., 2004. Characterization and source identification of a fine particle episode in Finland. Atmos. Environ. 38, 5003–5012.

Niemi, J.V., Tervahattu, H., Vehkamäki, H., Martikainen, J., Laakso, L., Kulmala, M., Aarnio, P., Koskentalo, T., Sillanpää, M., Makkonen, U., 2005. Characterization of aerosol particle episodes caused by wildfires in eastern Europe. Atmos. Chem. Phys. 5, 2299–2310.

Oberdörster, G., Oberdörster, E., Oberdörster, J., 2005. Nanotoxicology: an emerging discipline evolving from studies of ultrafine particles. Environ. Health Perspect. 113 (7), 823–839. https://doi.org/10.1289/ehp.7339.

Onasch, T.B., Trimborn, A., Fortner, E.C., Jayne, J.T., Kok, G.L., Williams, L.R., Davidovits, P., Worsnop, D.R., 2012. Soot particle aerosol mass spectrometer: Development, validation, and initial application. Aerosol Sci. Technol. 46, 804–817.

Paatero, P., Tapper, U., 1994. Positive matrix factorization – a nonnegative factor model with optimal utilization of error- estimates of data values. Environmetrics 5, 111–126.

Pirjola, L., Niemi, J.V., Saarikoski, S., Aurela, M., Enroth, J., Carbone, S., Saarnio, K., Kuuluvainen, H., Kousa, A., Rönkkö, T., Hillamo, R., 2017. Physical and chemical characterization of urban winter-time aerosols by mobile measurements in Helsinki, Finland. Atmos. Environ. 158, 60–75.

Ravindra, K., Sokhi, R., Grieken, R.V., 2008. Atmospheric polycyclic aromatic hydrocarbons: source Attribution, emission factors and regulation. Atmos. Environ. 42, 2895–2921.

Rolph, G., Stein, A., Stunder, B., 2017. Real-time environmental applications and display sYstem: READY. Environ. Model. Software 95, 210–228.

R Core Team, 2020. R: A Language and Environment for Statistical Computing. R Foundation for Statistical Computing, Vienna, Austria. URL. https://www.R-project.org/.

Saarikoski, S., Niemi, J.V., Aurela, M., Pirjola, L., Kousa, A., Rönkkö, T., Timonen, H., 2021. Sources of black carbon at residential and traffic environments obtained by two source apportionment methods. Atmos. Chem. Phys. 21, 14851–14869. https://doi.org/10.5194/acp-21-14851-2021.

Saarikoski, S., Sillanpää, M., Sofiev, M., Timonen, H., Saarnio, K., Teinilä, K., Karppinen, A., Kukkonen, J., Hillamo, R., 2007. Chemical composition of aerosols during a major biomass burning episode over northern Europe in spring 2006: experimental and modelling assessments. Atmos. Environ. 41 (17), 3577–3589. https://doi.org/10.1016/j.atmosenv.2006.12.053.

Saarikoski, S., Timonen, H., Saarnio, K., Aurela, M., Järvi, L., Keronen, P., Kerminen, V.-M., Hillamo, R., 2008. Sources of organic carbon in fine particulate matter in northern European urban air. Atmos. Chem. Phys. 8, 6281–6295.

Saarnio, K., Aurela, M., Timonen, M., Saarikoski, S., Teinilä, K., Mäkelä, T., Sofiev, M., Koskinen, J., Aalto, P.P., Kulmala, M., Kukkonen, J., Hillamo, R., 2010a. Chemical composition of fine particles in fresh smoke plumes from boreal wild-land fires in Europe. Sci. Total Environ. 408 (12), 2527–2542. https://doi.org/10.1016/j.scitotenv.2010.03.010.

Saarnio, K., Teinilä, K., Aurela, M., Timonen, H., Hillamo, R., 2010b. High-performance anion-exchange chromatography — mass spectrometry method for determination of levoglucosan, mannosan, and galactosan in atmospheric fine particulate matter. Anal. Bioanal. Chem. 398, 2253–2264.

Salo, L., Hyvärinen, A., Jalava, P., Teinilä, P., Hooda, R.K., Datta, A., Saarikoski, S., Lintusaari, H., Lepistö, T., Martikainen, S., Rostedt, A., Sharma, V.P., Rahman, M.H., Subudhie, S., Asmi, E., Niemi, J.V., Lihavainen, H., Lal, B., Keskinen, J., Kuuluvainen, H., Timonen, H., Rönkkö, T., 2021. The characteristics and size of lung-depositing particles vary significantly between high and low pollution traffic environments. Atmos. Environ. 255 https://doi.org/10.1016/j.atmosenv.2021.118421.

Sandradewi, J., Prévôt, A.S.H., Szidat, S., Perron, N., Alfarra, M.R., Lanz, V.A., Weingartner, E., Baltensperger, U., 2008. Using aerosol light absorption measurements for the quantitative determination of wood burning and traffic emission contributions to particulate matter. Environ. Sci. Technol. 42 (9), 3316–3323. https://doi.org/10.1021/es702253m, 42, 9, 3316–3323, 2008.

Schraufnagel, D.E., 2020. The health effects of ultrafine particles. Exp. Mol. Med. 52, 311–317. https://doi.org/10.1038/s12276-020-0403-3.

Shimada, K., Nochi, M., Yang, X., Sugiyama, T., Miura, K., Takami, A., Sato, K., Chen, X., Kato, S., Kajii, Y., Meng, F., Hatakeyama, S., 2020. Degradation of PAHs during long range transport based on simultaneous measurements at Tuoji Island, China, and at Fukue Island and Cape Hedo, Japan. Environ. Pollut. 260, 113906. https://doi.org/10.1016/j.envpol.2019.113906.

Shrivastava, M., Lou, S., Zelenyuk, A., Easter, R.C., Corley, R.A., Thrall, B.D., Rasch, P.J., Fast, J.D., Simonich, S.L.M., Shen, H., Tao, S., 2017. Global long-range transport and lung cancer risk from polycyclic aromatic hydrocarbons shielded by coatings of organic aerosol. Natl. Acad. Sci. 114 (6), 1246e1251.

Soares, J., Kousa, A., Kukkonen, J., Matilainen, L., Kangas, L., Kauhaniemi, M., Riikonen, K., Jalkanen, J.-P., Rasila, T., Hänninen, O., Koskentalo, T., Aarnio, M., Hendriks, C., Karppinen, A., 2014. Refinement of a model for evaluating the population exposure in an urban area. Geosci. Model Dev. (GMD) 7, 1855–1872.

Stein, A.F., Draxler, R.R., Rolph, G.D., Stunder, B.J.B., Cohen, M.D., Ngan, F., 2015. NOAA's HYSPLIT atmospheric transport and dispersion modeling system. Bull. Am. Meteorol. Soc. 96, 2059–2077.

Teinilä, K., Aurela, M., Niemi, J.V., Kousa, A., Petäjä, T., Järvi, L., Hillamo, R., Kangas, L., Saarikoski, S., Timonen, H., 2019. Concentration variation of gaseous and particulate pollutants in the Helsinki city centre — observations from a two-year campaign from 2013–2015. BER 24, 115–136.

Tissari, J., Lyyr€anen, J., Hyt€onen, K., Sippula, O., Tapper, U., Frey, A., Saarnio, K., Pennanen, A.S., Hillamo, R., Salonen, R.O., et al., 2008. Fine particle and gaseous emissions from normal and smouldering wood combustion in a conventional masonry heater. Atmos. Environ. 42 (34), 7862–7873. https://doi.org/10.1016/j.atmosenv.2008.07.019.

Ulbrich, I.M., Canagaratna, M.R., Zhang, Q., Worsnop, D.R., Jimenez, J.L., 2009. Interpretation of organic components from Positive Matrix Factorization of aerosol mass spectrometric data. Atmos. Chem. Phys. 9, 2891–2918.

Vestenius, M., Leppänen, S., Anttila, P., Kyllönen, K., Hatakka, J., Hellén, H., Hyvärinen, A.-P., Hakola, H., 2011. Background concentrations and source apportionment of polycyclic aromatic hydrocarbons in south-eastern Finland. Atmos. Environ. 45 (20), 3391–3399. https://doi.org/10.1016/j.atmosenv.2011.03.050.

Zanobetti, A., Austin, E., Coull, B.A., Schwartz, J., Koutrakis, P., 2014. Health effects of multi-pollutant profiles. Environ. Int. 71, 13–19.

Zotter, P., Herich, H., Gysel, M., El-Haddad, I., Zhang, Y., Močnik, G., Hüglin, C., Baltensperger, U., Szidat, S., Prévôt, A.S.H., 2017. Evaluation of the absorption Ångström exponents for traffic and wood burning in the Aethalometer-based source apportionment using radiocarbon measurements of ambient aerosol. Atmos. Chem. Phys. 17, 4229–4249.